# Free-surface Effect on Tidal Turbine Performance

JinhuiYan, Ph.D., Assistant Professor
Department of Civil and Environmental Enginering

University of Illinois at Urbana-Champaign
Urbana, USA
yjh@illinois.edu

***Abstract***: In this paper, the quantitative investigation of the free-surface effect on tidal turbine performance by using a multi-phase flow formulation is presented. The computational formulation is briefly introduced. The free-surface effect is rigorously studied by the simulations performed for a single turbine and two back-to-back turbines using different inflow conditions and immersion depths. The thrust and power coefficients of the tidal turbines in free-surface flows are quantified. It is found that the presence of free-surface has a significantly negative effect on tidal turbine performance by decreasing the thrust and power coefficients in idealized inflow conditions, such as uniform inflow and Airy wave inflow conditions. The comparison with pure hydrodynamics simulation results shows that pure hydrodynamics simulations are unable to provide accurate predictions and the free-surface effect must be taken into account in the modeling and simulations of tidal turbines, especially for shallow immersion depth.

*Keywords—tidal energy, computational fluid dynamics, free-surface flows*

## I. Introduction

Tidal energy is a more predictable renewable energy source, compared with wind and tidal energy, which heavily rely on the weather. Tidal turbine has been proved to be an effective energy harvesting device that can extract electricity from waves and tides [1]. In the design and optimization of tidal turbines, computational fluid dynamics (CFD) simulations have been playing an important role in quantifying the hydrodynamics loads on the tidal turbines and complicated flow-turbine interaction. Nowadays, a lot of numerical simulations can be in the literature, and most of them utilized the single-phase CFD techniques that are commonly used in wind energy. Although these techniques can be directly applied to tidal turbine simulations by changing the fluid property, none of these simulations considered the free-surface effect [2-7], which has been proved by several experiments in [8,9] to be non-negligible. Thus, the paper presents a rigorous quantitative investigation of the free-surface effect on tidal turbine performance by using a novel multi-phase flow solver. The focus is placed on the thrust and power coefficients, which are the most engineering quantities for tidal turbine performance. Both single turbine and two back-to-back turbines are simulated by using both pure hydrodynamics and free-surface simulations. For the single turbine configuration, the simulations are performed by using both uniform inflow conditions and Airy wave inflow conditions with different immersion depths. For two back-to-back turbine simulations, the wake effect on the downstream turbine is also quantified.

## II. Numerical Methods

The level set method [10-14] is utilized to model the free-surface flows around tidal turbines. In level set method, the air-water interface (free-surface) is distinguished by a level set field, $\varphi$, which is governed by the following convection equation

$$\frac{\partial \varphi}{\partial t} + \vec{u} \cdot \nabla \varphi = 0 \qquad (1)$$

where $\vec{u}$ is the fluid velocity vector. The motion of the free-surface flow is governed by the following unified two-phase Navier-Stokes equation of incompressible flows,

$$\rho(\varphi)\left(\frac{\partial \vec{u}}{\partial t} + \vec{u} \cdot \nabla \vec{u} - \vec{g}\right) + \nabla p - 2\mu(\varphi)\nabla \vec{u} = \vec{0} \qquad (2)$$

$$\nabla \cdot \vec{u} = 0 \qquad (3)$$

where $p$ is the fluid pressure, the fluid density $\rho$ and viscosity $\mu$ are interpolated by the density and viscosity of air and water, namely,

$$\rho(\varphi) = \rho_a[1 - H(\varphi)] + \rho_w H(\varphi)$$

$$\mu(\varphi) = \mu_a[1 - H(\varphi)] + \mu_w H(\varphi)$$

where $H(\varphi)$ is a Heaviside function based on the level set field.

The coupled partial differential equations (PDEs) in Eq. (1)-(3), together with appropriate initial and boundary conditions, describe free-surface flow at the continuous level. In the present work, an arbitrary Lagrangian-Eulerian variational multi-scale formulation (ALE-VMS) [15-17], which acts as a large eddy simulation model (LES), and weak enforcement of essential boundary condition (Weak BC) [18-20], which acts a wall model, are utilized to solve the coupled PDEs in a fully coupled fashion. A re-initialization based on Eikonal equation and mass balancing level set technique is also incorporated into the computational framework. To enable the "full machine" simulation, where both the rotor and tower are included, the sliding interface technique is adopted to handle the relative motion between the spinning rotor and stationary tower [21-23]. This computational framework has been validated in our previous work. It has been successfully applied to the fluid-structure interaction analysis of offshore floating wind turbines [24]. More details about numerical methods, including time integration and linear solvers, can be found in [25].

## III. Single turbine simulations using uniform inflow condition

In this section, a single tidal turbine is simulated by using a uniform inflow condition. The turbine simulated here are taken from [9], which has three blades with a diameter $D$ = 0.8 m and a pitch angle of 20°. A CAD model of the turbine rotor is shown in Fig. 1.

The problem setup is depicted in Fig. 2. Two immersion depths are considered, which have also been experimentally studied in [9]. Fig. 3 and Fig. 4 shows the flow structure colored by the velocity magnitude in the fully developed stage from pure hydrodynamics and free-surface simulations. After the flow hits the tower, the free-surface undergoes large deformation, and a large amount of the tip vortex is generated due to the rotation of the turbine rotor.

We report the thrust coefficient $C_T$ and power coefficient $C_P$. The definition of $C_T$ and $C_P$ are defined as $C_T = \frac{4F}{0.5\rho\pi D^2 U^2}$ and $C_P = \frac{4T\Omega}{0.5\rho\pi D^2 U^3}$, where $F$ and $T$ are the hydrodynamic thrust force and torque, respectively, $U$ is the incoming water speed. Here $U$ = 1.5 m/s is used. Fig. 3 shows the time history of thrust coefficient $C_T$ and power coefficient $C_P$ predicted by both free-surface and pure hydrodynamics simulations. The experimental data obtained from [9] is also plotted for the comparison. The $C_T$ and $C_P$ predicted by free-surface simulations are in good agreement with experimental data for both shallow and deep immersion cases. One notable trend is that the $C_T$ and $C_P$ are higher in deep immersion case, which can be seen from both free-surface simulations and the experiments. It can be also seen that the $C_T$ and $C_P$ predicted by pure hydrodynamics simulation is very similar to the deep immersion case, which indicates that free-surface effect is not important in the deep immersion case but non-negligible in the shallow immersion case.

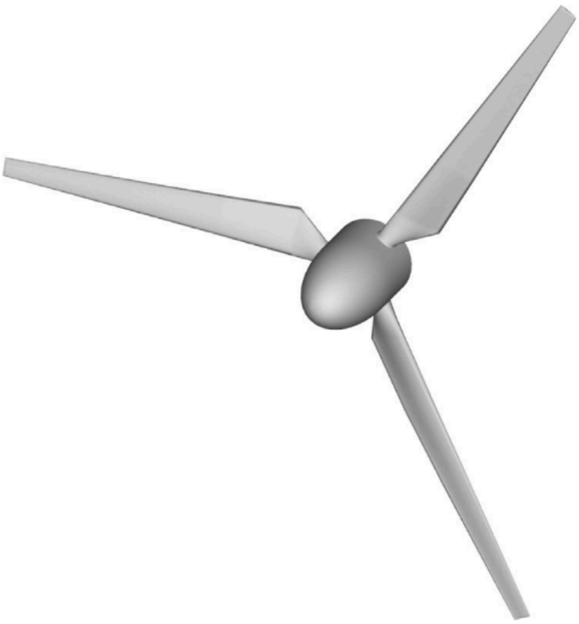

Fig. 1. Tidal turbine surface model employed in the present work.

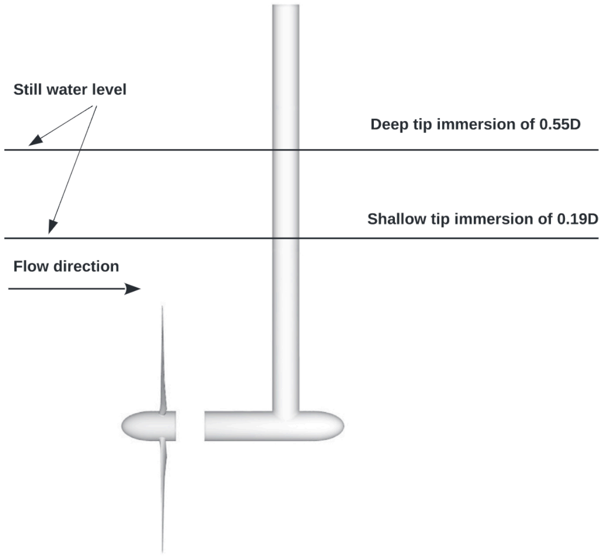


Fig. 2. Problem setup of single turbine simulations.

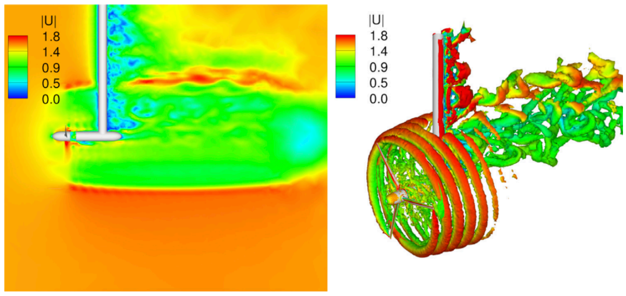


Fig. 3. Pure hydrodynamics simulation. Left: Velocity (in m/s) on a planar cut. Right: Vorticity colored by velocity magnitude (in m/s).

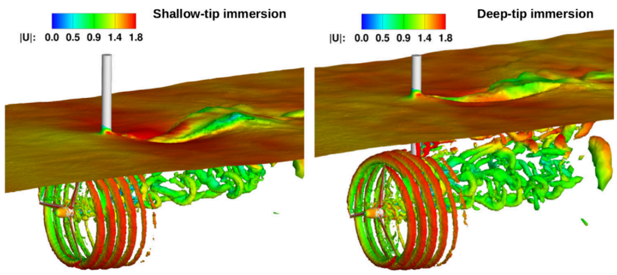


Fig. 4. Free-surface deformation and vorticity colored by velocity magnitude (in m/s) of single turbine simulation using uniform inflow condition.

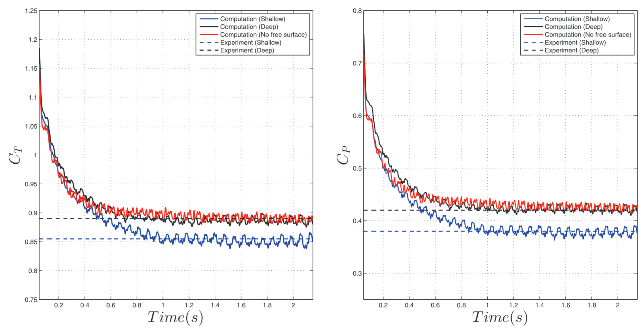


Fig. 5. Time history of $C_T$ and $C_p$ of single turbine simulations using uniform inflow condition.

## IV. Single turbine simulation using an Airy wave inflow condition

To further investigate the free-surface effect, a single turbine is simulated by using an Airy wave inflow. The wave height and wavelength are set to 0.085 m and 2.4 m, respectively. In addition to the previous shallow and deep cases, an intermediate immersion case is simulated. The free-surface and tip vorticity colored by velocity magnitude for the three cases is shown in Fig. 6. More complicated flow behavior and interaction between free-surface and tip vorticity are observed in the simulations. Fig. 4 shows the time history of $C_T$ and $C_P$. The averaged values in the fully developed stage are summarized in Table I. Large fluctuations of $C_T$ and $C_P$ are observed in the presence of waves. However, the averaged values still show that as the turbine is placed closer to the free-surface, both $C_T$ and $C_P$ decrease, which indicates the presence of free-surface has a negative effect on the tidal turbine performance. It is also seen that the averaged $C_T$ and $C_P$ between the medium immersion and deep immersion cases are very similar, suggesting the existence of a minimum depth at which the tidal turbine will operate to their full potential.

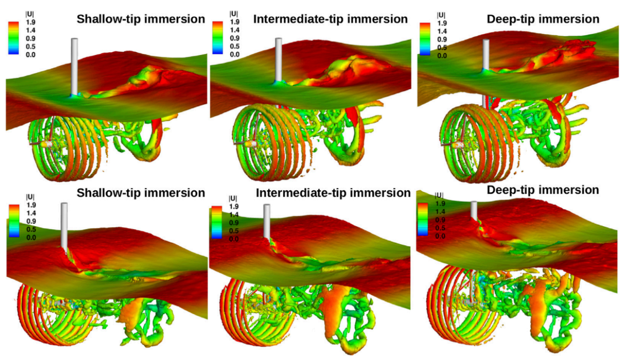


Fig. 6. Free-surface deformation and vorticity colored by velocity magnitude (in m/s) of single turbine simulations using an Airy wave inflow condition.

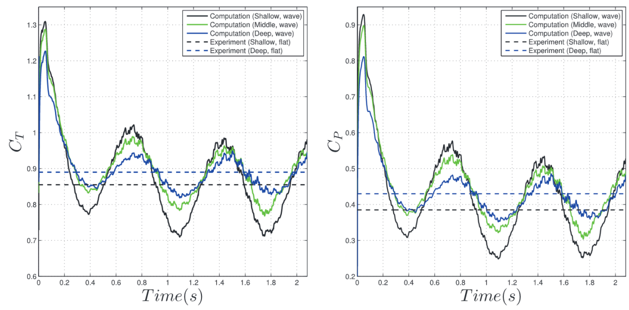


Fig. 7. Time history of $C_T$ and $C_p$ of single turbine simulations using an Airy wave inflow condition.

TABLE I. Predicted averaged $C_T$ and $C_P$ of single turbine simulation using Airy wave inflow condition.

| Cases | $\overline{C_T}$ | $\overline{C_P}$ |
|---|---|---|
| Shallow immersion | 0.8513 | 0.3919 |
| Intermediate immersion | 0.8741 | 0.4141 |
| Deep immersion | 0.8794 | 0.4144 |

## V. Two back-to-back simulations

In the previous section, it is proved that free-surface has a negative effect on the tidal turbine performance, but the effect is negligible in the deep immersion case. In this section, two back-to-back turbines are simulated by using the deep immersion in the previous section with a uniform inflow condition. The goal is trying to answer the following two questions: 1. How much is the efficiency drop of the downstream turbine? 2. Is free-surface effect significant for this two back-to-back turbine configuration, given the fact that the free-surface effect is not important for a single turbine with this immersion depth?

The problem setup is shown in Fig. 8, where the distance between the upstream turbine and downstream turbine is $L$ = 3.5 m. Both free-surface simulation and pure hydrodynamics simulation are performed to quantify the free-surface effect.

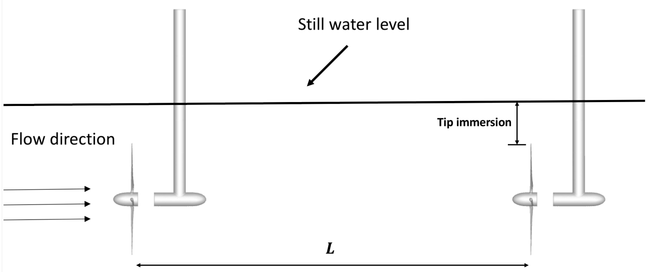


Fig. 8. Problem setup of two back-to-back turbine simulations.

The time history of $C_T$ and $C_P$ is showed in Fig. 9. The thrust and power coefficients of the upstream turbine still stay at the same level as the single turbine configuration. Higher-amplitude fluctuations of thrust and power coefficients for the downstream turbine are observed due to the turbulent wake generated by the upstream turbine. The comparison of $C_T$ and $C_P$ between free-surface and pure hydrodynamics simulations is shown in Fig. 10. It shows that the free-surface effect is still negligible for the upstream turbine. Free-surface and pure hydrodynamics simulations produce quite similar predictions for $C_T$ and $C_P$ for the upstream turbine. However, the pure hydrodynamics simulation predicts much higher $C_T$ and $C_P$ than the free-surface simulation for the downstream turbine.

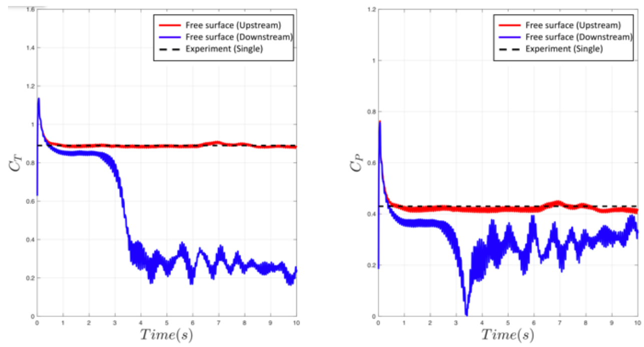


Fig. 9. Time history of $C_T$ and $C_p$ of two back-to-back turbines simulations.

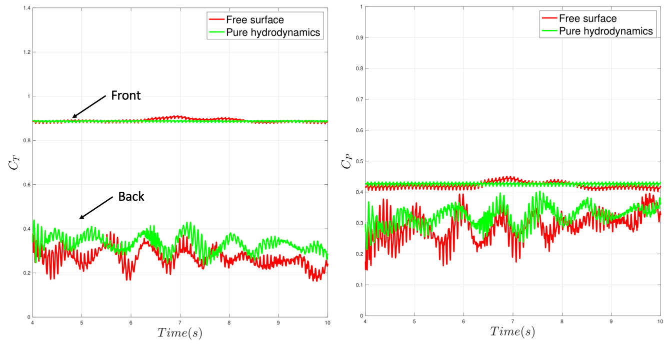


Fig. 10. Time history of $C_T$ and $C_P$ of two back-to-back turbines simulations.

Table II summarizes the averaged $C_T$ and $C_P$ for both free-surface and pure hydrodynamics simulations for the upstream and downstream turbines. The averaged thrust and power coefficients of the upstream turbine predicted by the pure hydrodynamics and the free-surface flow simulations are quite similar, still agreeing with experimental data [9] based on a single turbine. The thrust and the power coefficients of the downstream turbine are only 30% and 62.3% of that of the upstream turbine, respectively. Besides, the pure hydrodynamics simulation predicts higher coefficients than the free-surface flow simulation does for the downstream turbine. The discrepancy between the pure hydrodynamics simulation and the free-surface flow simulation is 7% for thrust coefficient and 15% for power coefficient.

TABLE II. PREDICTED AVERAGED $C_T$ AND $C_P$ OF TWO BACK-TO-BACK TURBINES SIMULATIONS.

| Cases | $\overline{C_T}$ | $\overline{C_P}$ |
|---|---|---|
| Free-surface (upstream) | 0.8894 | 0.4216 |
| Hydrodynamics (upstream) | 0.8902 | 0.4263 |
| Free-surface (downstream) | 0.2698 | 0.2886 |
| Hydrodynamics (downstream) | 0.2886 | 0.3308 |

The water speed between the two turbines averaged over 10 rotor revolutions are plotted in Fig. 11 at different locations as a function of the radial coordinate. A short distance past the upstream turbine the profile appears distorted from a uniform profile. As going to downstream, the average water speed at a specified radial coordinate decreases. It is also observed that the averaged water speed at a specified radial coordinate is lower in the free-surface flow simulation, which explains why smaller thrust and power coefficients are predicted by the free-surface flow simulation. These findings indicate that the free-surface does not affect the upstream tidal turbine too much but significantly change the performance of the downstream turbine in the current turbine arrangement.

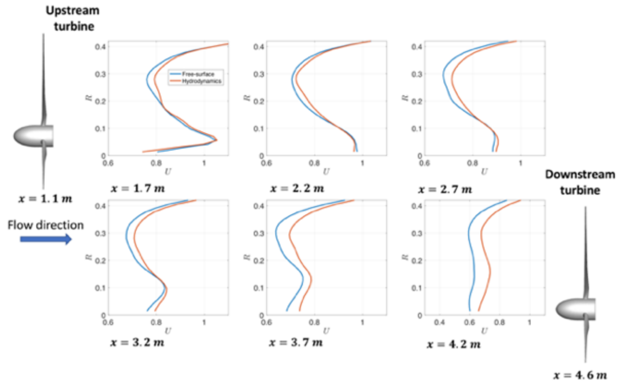


Fig. 11. Water speed between the two turbines averaged over 10 rotor revolutions plotted at different locations as a function of the radial coordinate.

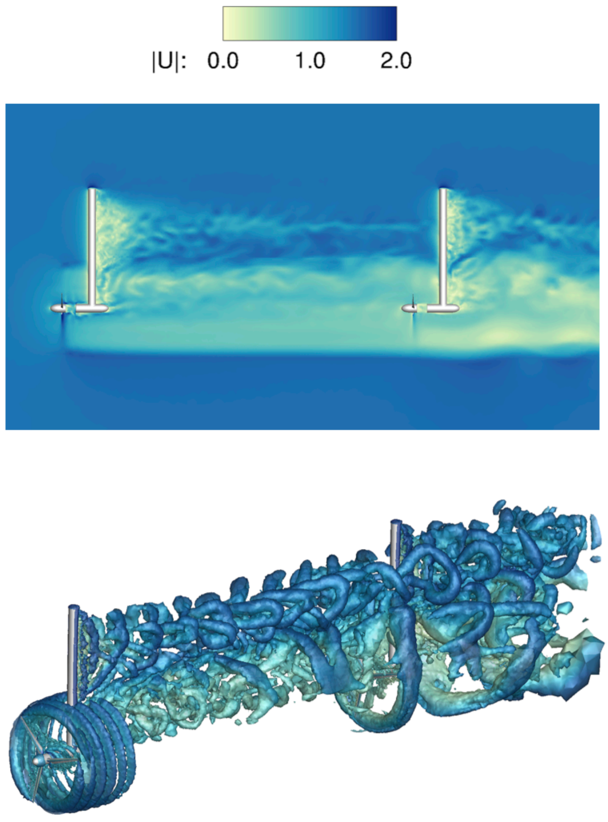


Fig. 12. Velocity magnitude (in m/s) on a planar cut and vorticity colored by velocity magnitude (in m/s) of pure hydrodynamics simulation of two back-to-back turbines.

Fig. 12 shows the vorticity isosurfaces colored velocity magnitude from pure hydrodynamics simulation. Fig. 13 shows the free-surface and tip vorticity colored by the velocity magnitude. As going downstream, it is observed that the interaction between tip vortex and free-surface becomes more and more pronounced, resulting in substantial the air-water interface deformation, which produces more pronounced free-surface effect on the thrust and power coefficients of the downstream turbine partially because some amount of kinetic energy goes to excite the free-surface motion.

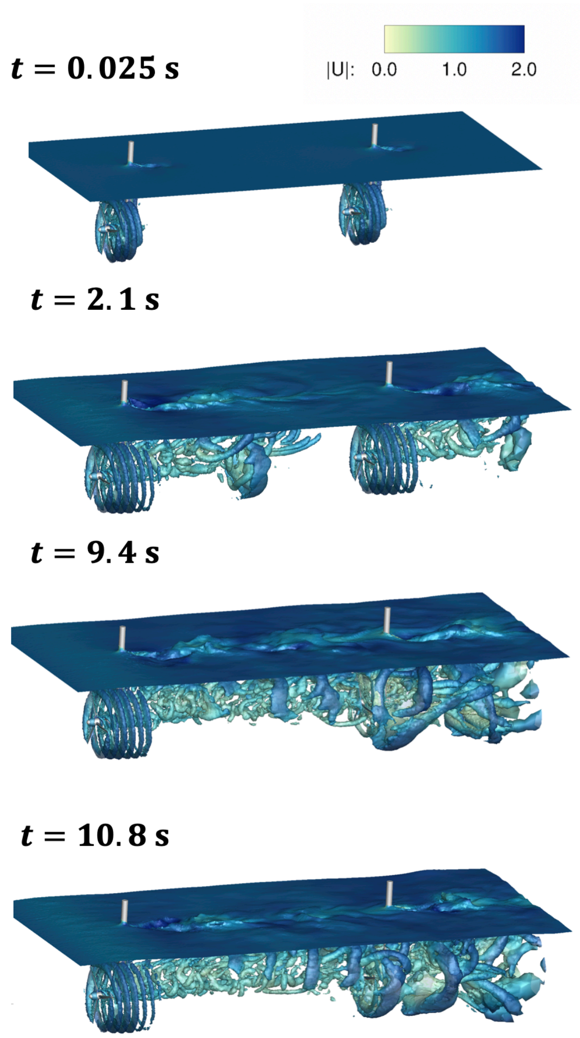


Fig. 13. Free-surface deformation and tip vorticity colored by velocity magnitude (in m/s) of two back-to-back turbines simulation using a uniform inflow condition.

## VI. CONCLUSION

A computational multi-phase flow framework is used to investigate the free-surface effect on tidal turbine performance. The simulations are carried out at full-scale and with the full complexity of tidal turbine component geometry. Without any empiricism, the simulations can accurately capture hydrodynamic loading on the tidal turbine and the free-surface effect on the tidal turbine performance under different inflow conditions.

For single turbine simulations, both a uniform inflow condition and an Airy wave inflow conditions are considered. It was found the free-surface has a negative effect on the tidal turbine performance under these idealized inflow conditions. The thrust and power coefficients are higher in the deep immersion case. These computations also revealed the presence of a minimum immersion depth for optimal operation of the tidal turbine.

Two back-to-back turbines are further simulated by using the deep-immersion operating conditions. It was found that a drop in thrust coefficient of 70% and a drop of power coefficient of 38.7% between the upstream and downstream turbines are predicted by the free-surface simulations. By comparing the results of the pure hydrodynamics simulation and free-surface simulation, it is found that the free-surface does not affect the upstream turbine but significantly change the performance of the downstream turbine. The discrepancy between the pure hydrodynamics simulation and the free-surface flow simulation is 7% for thrust coefficient and 15% for power coefficient for the downstream. All of these findings indicate that accurate simulations are only possible if the free-surface effect is properly modeled.

This work is a first step in using full-scale free-surface flow simulations of tidal turbines with full geometry details. We also plan to extend the current methodology to simulate tidal farm arranged in arrays. Fluid-structure interaction (FSI) effect and cavitation will be considered in future research.

## ACKNOWLEDGMENT

The simulations are performed in Texas Advanced Computing Center (TACC). The computing resources are greatly acknowledged.

## REFERENCES

[1] Goundar, Jai N., and M. Rafiuddin Ahmed. "Design of a horizontal axis tidal current turbine." Applied energy 111 (2013): 161-174.

[2] Baltazar, J., & De Campos, J. F. (2011). Hydrodynamic analysis of a horizontal axis marine current turbine with a boundary element method. Journal of Offshore Mechanics and Arctic Engineering, 133(4), 041304.

[3] Lee, J. H., Park, S., Kim, D. H., Rhee, S. H., & Kim, M. C. (2012). Computational methods for performance analysis of horizontal axis tidal stream turbines. Applied Energy, 98, 512-523.

[4] Li, Y., & Calisal, S. M. (2010). Three-dimensional effects and arm effects on modeling a vertical axis tidal current turbine. Renewable energy, 35(10), 2325-2334.

[5] Malki, R., Williams, A. J., Croft, T. N., Togneri, M., & Masters, I. (2013). A coupled blade element momentum–Computational fluid dynamics model for evaluating tidal stream turbine performance. Applied Mathematical Modelling, 37(5), 3006-3020.

[6] Masters, I., Chapman, J. C., Willis, M. R., & Orme, J. A. C. (2011). A robust blade element momentum theory model for tidal stream turbines including tip and hub loss corrections. Journal of Marine Engineering & Technology, 10(1), 25-35.

[7] Zhu, Q., & Yan, J. (2019). A moving-domain CFD solver in FEniCS with applications to tidal turbine simulations in turbulent flows. Computers & Mathematics with Applications.

[8] Bahaj, A. S., W. M. J. Batten, and G. McCann. "Experimental verifications of numerical predictions for the hydrodynamic performance of horizontal axis marine current turbines." Renewable energy 32.15 (2007): 2479-2490.

[9] Bahaj, A. S., Molland, A. F., Chaplin, J. R., & Batten, W. M. J. (2007). Power and thrust measurements of marine current turbines under various hydrodynamic flow conditions in a cavitation tunnel and a towing tank. Renewable energy, 32(3), 407-426.

[10] Akkerman, I., Dunaway, J., Kvandal, J., Spinks, J., & Bazilevs, Y. (2012). Toward free-surface modeling of planing vessels: simulation of the Fridsma hull using ALE-VMS. Computational Mechanics, 50(6), 719-727.

[11] Akkerman, I., Bazilevs, Y., Benson, D. J., Farthing, M. W., & Kees, C. E. (2012). Free-surface flow and fluid-object interaction modeling with emphasis on ship hydrodynamics. Journal of Applied Mechanics, 79(1), 010905.

[12] Kees, C. E., Akkerman, I., Farthing, M. W., & Bazilevs, Y. (2011). A conservative level set method suitable for variable-order approximations and unstructured meshes. Journal of Computational Physics, 230(12), 4536-4558.

[13] Yan, J., Yan, W., Lin, S., & Wagner, G. J. (2018). A fully coupled finite element formulation for liquid–solid–gas thermo-fluid flow with melting and solidification. Computer Methods in Applied Mechanics and Engineering, 336, 444-470.

[14] Lin, S., Yan, J., Kats, D., & Wagner, G. J. (2019). A volume-conserving balanced-force level set method on unstructured meshes

using a control volume finite element formulation. Journal of Computational Physics, 380, 119-142.

[15] Bazilevs, Y., Hsu, M. C., Takizawa, K., & Tezduyar, T. E. (2012). ALE-VMS and ST-VMS methods for computer modeling of wind-turbine rotor aerodynamics and fluid–structure interaction. Mathematical Models and Methods in Applied Sciences, 22(supp02), 1230002.

[16] Bazilevs, Y., Takizawa, K., Tezduyar, T. E., Hsu, M. C., Kostov, N., & McIntyre, S. (2014). Aerodynamic and FSI analysis of wind turbines with the ALE-VMS and ST-VMS methods. Archives of Computational Methods in Engineering, 21(4), 359-398.

[17] Takizawa, K., Bazilevs, Y., & Tezduyar, T. E. (2012). Space–time and ALE-VMS techniques for patient-specific cardiovascular fluid–structure interaction modeling. Archives of Computational Methods in Engineering, 19(2), 171-225.

[18] Bazilevs, Y., Calo, V. M., Cottrell, J. A., Hughes, T. J. R., Reali, A., & Scovazzi, G. (2007). Variational multiscale residual-based turbulence modeling for large eddy simulation of incompressible flows. Computer methods in applied mechanics and engineering, 197(1-4), 173-201.

[19] Bazilevs, Y., & Hughes, T. J. (2007). Weak imposition of Dirichlet boundary conditions in fluid mechanics. Computers & Fluids, 36(1), 12-26.

[20] Bazilevs, Y., Michler, C., Calo, V. M., & Hughes, T. J. R. (2010). Isogeometric variational multiscale modeling of wall-bounded turbulent flows with weakly enforced boundary conditions on unstretched meshes. Computer Methods in Applied Mechanics and Engineering, 199(13-16), 780-790.

[21] Yan, J., Deng, X., Korobenko, A., & Bazilevs, Y. (2017). Free-surface flow modeling and simulation of horizontal-axis tidal-stream turbines. Computers & Fluids, 158, 157-166.

[22] Yan, J., Augier, B., Korobenko, A., Czarnowski, J., Ketterman, G., & Bazilevs, Y. (2016). FSI modeling of a propulsion system based on compliant hydrofoils in a tandem configuration. Computers & Fluids, 141, 201-211.

[23] Bazilevs, Y., & Hughes, T. J. R. (2008). NURBS-based isogeometric analysis for the computation of flows about rotating components. Computational Mechanics, 43(1), 143-150.

[24] Yan, J., Korobenko, A., Deng, X., & Bazilevs, Y. (2016). Computational free-surface fluid–structure interaction with application to floating offshore wind turbines. Computers & Fluids, 141, 155-174.

[25] Yan, J. (2016). Computational free-surface fluid-structure interaction with applications on offshore wind and tidal energy (Doctoral dissertation, UC San Diego).